

Controlling dielectric and pyroelectric properties of compositionally graded ferroelectric rods by an applied pressure

Yue Zheng and C. H. WooBiao Wang

Citation: [Journal of Applied Physics](#) **101**, 116103 (2007); doi: 10.1063/1.2736308

View online: <http://dx.doi.org/10.1063/1.2736308>

View Table of Contents: <http://aip.scitation.org/toc/jap/101/11>

Published by the [American Institute of Physics](#)

AIP | Journal of
Applied Physics

Save your money for your research.
It's now **FREE** to publish with us -
no page, color or publication charges apply.

Publish your research in the
Journal of Applied Physics
to claim your place in applied
physics history.

Controlling dielectric and pyroelectric properties of compositionally graded ferroelectric rods by an applied pressure

Yue Zheng^{a)} and C. H. Woo^{b)}

Department of Electronic and Information Engineering, The Hong Kong Polytechnic University, Hong Kong SAR, China

Biao Wang^{c)}

Electro-Optics Technology Center, Harbin Institute of Technology, Harbin, 150001, China

(Received 12 February 2007; accepted 22 March 2007; published online 4 June 2007)

The polarization, charge offset, dielectric, and pyroelectric properties of a compositionally graded ferroelectric rod inside a high-pressure polyethylene tube are studied using a thermodynamic model based on the Landau-Ginzburg-Devonshire formulation. The calculated distribution of the polarization in the rod is nonuniform, and the corresponding charge offset, dielectric, and pyroelectric properties vary according to the applied pressure. This behavior may be used as a convenient means to control these properties for design optimization. © 2007 American Institute of Physics. [DOI: 10.1063/1.2736308]

The use of graded ferroelectrics is essential in many applications, such as tunable microwave devices, transcapacitors, and other dielectric devices.^{1–9} Distribution of the polarization in these materials is asymmetric and graded, and the hysteresis loop is not centrosymmetric, but displaced along the polarization axis, giving rise to an attendant charge offset. Properties such as the effective pyroelectric response, temperature dependence of the dielectric behavior, etc.^{1,3} vary with the degree of asymmetry.

Graded ferroic material systems studied recently are not restricted to cases where the gradient is in the composition, but include also those in which gradients also exist in the temperature and/or stress. Ban *et al.*⁴ used a generalized Landau-Ginzburg model to study the offset hysteresis of polarization-graded ferroelectric materials, and found that the internal elastic energy due to the spatial variation of the self-strain tends to flatten the polarization distribution. The nonuniform polarization thus produced may then yield an asymmetrical hysteresis with “up” or “down” charge offset. Zhong *et al.*^{1,3} investigated the pyroelectric response and dielectric permittivity of compositionally graded ferroelectric material, and found that the effective pyroelectric coefficients were directly related to the compositional gradient of the system. The effects on the polarization and charge offset of a ferroelectric due to a compression gradient normal to the substrate have also been studied.⁶ Imposing a temperature gradient across ferroelectric materials, Fellberg *et al.*⁷ observed up and down hysteresis offsets, similar to those found in polarization-graded ferroelectrics.

In this article, the polarization, charge offset, dielectric, and pyroelectric properties of a compositionally graded ferroelectric rod inside a high-pressure polyethylene tube are considered. The calculations follow a thermodynamic approach based on the Landau-Ginzburg-Devonshire (LGD) model. The results are used to speculate on the feasibility of design optimization by adjusting the applied pressure.

We consider a rod of compositionally graded ferroelectric (CGFR) material with radius R and height h , sandwiched between electrodes at both ends, and placed inside a high-pressure polyethylene (HPPE) tube.⁸ A stiff steel cylindrical housing (SH) contains the HPPE tube and CGF rod. Moreover, two thin electrodes were sputter-deposited onto the surfaces perpendicular to CGFR's length.⁹ We call the arrangement an S-H-C system. We consider the rod homogeneous along the x and y directions such that $P_1=P_2=0$ and $P_3=P(z)$.

The linear elastic stress-strain relations in the HPPE under an applied axial pressure along the z -direction are given by $\varepsilon_r=[(1-\nu)\sigma_r-\nu\sigma_z]/E$ and $\varepsilon_z=(\sigma_z-2\nu\sigma_r)/E$, where E and ν are Young's modulus and Poisson's ratio of the HPPE, respectively. σ_z is the applied axial load, and σ_r is the corresponding radial stress. ε_z and ε_r are the axial and radial strain, respectively. Since the CGF rod and SH are much stiffer than the HPPE, we have $\varepsilon_r=0$, and the radial stress can be written as $\sigma_r=\nu/(1-\nu)\sigma_z=-(\nu/1-\nu)p$, where p is value of applied axial pressure. We note that the CGFR tube considered here has a length much larger than its radius, i.e., $h \gg R$, so that the bending moment on CGFR due to the interfacial mismatch can be neglected and all the internal stresses come from the transformation strain.⁴ The total free energy of CGFR is composed of the Landau energy, depolarization energy, electrostrictive energy, and elastic energy. With the radial compressive stress contribution, the total free energy of the rod can be written in the cylindrical coordinates (r, φ, z) , following Refs. 1, 10, and 11,

^{a)}On leave from Electro-Optics Technology Center, Harbin Institute of Technology, Harbin, 150001, China.

^{b)}Corresponding author; electronic mail: chung.woo@polyu.edu.hk

^{c)}Also at: State and Key Laboratory of Optoelectronic Materials and Technologies, Institute of Optoelectronic and Functional Composite Materials and School of Physics and Engineering, Sun Yat-sen University, Guangzhou, China.

$$F = 2\pi \int_0^h dz \int_0^R r dr \left\{ \frac{\alpha(z)}{2} (T - T_{c0}) P^2(z) + \frac{\beta(z)}{4} P^4(z) + \frac{\gamma(z)}{6} P^6(z) + \frac{D}{2} [\nabla P(z)]^2 - \frac{1}{2} E_d(z) P(z) - E_{\text{ext}} P(z) - 2\sigma_r \varepsilon_0(z) - [s_{11}(z) + s_{12}(z)] \sigma_r^2 \right\}, \quad (1)$$

where α is proportional to the inverse Curie constant regarded known for the bulk material. α , β , γ , and D are the free-energy expansion coefficients of the corresponding bulk material. The coupling effect between the mechanical deformation and the polarization can be expressed using the electrostrictive coefficient Q_{12} , and the self-strain induced by the polarization can be written as $\varepsilon_0(z) = Q_{12} P(z)^2$. s_{11} and s_{12} are components of the elastic compliance tensor.⁴ $E_d(z)$ is the depolarization field, which has been discussed in the literature.^{1,4} $E_{\text{ext}}(z)$ is the external field.

In the absence of an applied electric field ($E_{\text{ext}}=0$), optimizing the total free energy with respect to the polarization field yields the Euler-Lagrange equation $\delta F / \delta P = 0$, through which the stationary values of P can be solved.¹⁰⁻¹⁴ In the present analysis, the rod is assumed to be sufficiently thick so that effects of lattice relaxation on all surfaces of the rod can be neglected. The boundary conditions are assumed to satisfy $\partial P / \partial z = 0$ at $z=0$ and $z=h$, corresponding to a complete charge compensation¹ on the interface between the ferroelectric and the substrates. This boundary condition is equivalent to setting the extrapolation lengths on the end surfaces of the ferroelectric rod to infinity, i.e., $\delta_0 = \delta_h \rightarrow \infty$. Without this assumption, the boundary conditions must yield $\partial P / \partial z = \mp P / \delta_{u-b}$, for $z=0$ and $z=h$, $\partial P / \partial z = -P / \delta_{s-w}$ for $r=R$, δ_{u-b} and δ_{s-w} are the extrapolation lengths of the polarization on the end surfaces and the sidewall, respectively.¹ We also follow other authors,^{1,4} to assume that the contribution of the depolarization field is negligible when the compositional gradient across the ferroelectric rod is smooth.

In the following, we consider a rod of the CGF material $\text{Ba}_m\text{Sr}_{1-m}\text{TiO}_3$ (BST), with the composition at one end fixed at BT, and the other one at a composition of BT-BST 70/30. The material constants we use, such as the electrostrictive coefficients and the elastic coefficients of BaTiO_3 , SrTiO_3 , and BST, are taken from Refs. 4 and 15 and listed in Ref. 16.

Figure 1(a) shows the polarization profiles in CGFR as a function of applied axial compressive stress ($\sigma_z=0, -0.25, -0.5, -1, -2$ GPa) on the HPPE. Enhancement of the polarization by the axial compressive stress can be clearly seen. The corresponding normalized polarization profiles in Fig. 1(b) further show the increasing heterogeneity of the polarization field with increasing axial compressive stresses in our S-H-C system. The dielectric susceptibility of the CGF rod can be calculated as a function of location from the polarization change ΔP due to an applied electric field E as

$$\chi(z) = \frac{1}{\varepsilon_0} \frac{\Delta P}{E}. \quad (2)$$

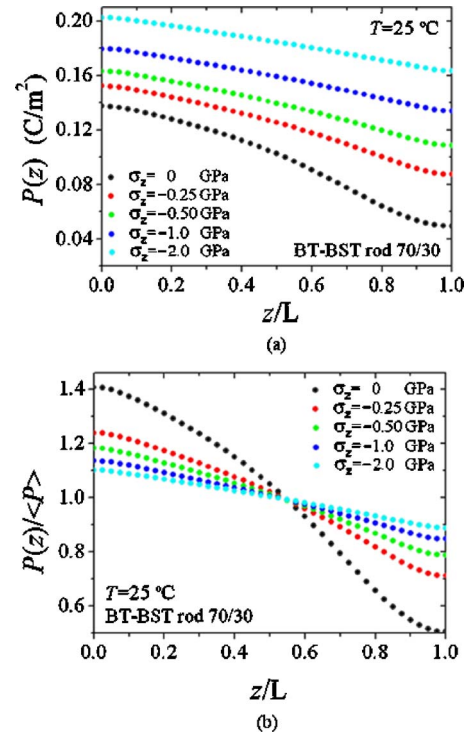


FIG. 1. (Color online) (a) Polarization profile, (b) Normalized polarization profiles of the BST (70/30) CGFR in S-H-C system for different applied pressure.

At the same time, the spatially averaged susceptibility χ_m of the rod is given by

$$\chi_m = \frac{L}{\int_0^h \{1/[\chi(z) + 1]\} dz} - 1. \quad (3)$$

Figure 2 shows χ_m as a function of temperature for various applied pressures. Instead of the sharp peak in a homogeneous bulk ferroelectric, the dielectric susceptibility of the CGF rod is a more moderately peaked function of temperature. The broadening of the peak is due to composition gradient. At the same time, the dielectric behavior as reflected in both the magnitude and position of the susceptibility peak can be seen to be effectively controlled by the applied pressure. A high dielectric susceptibility, if desirable, can be

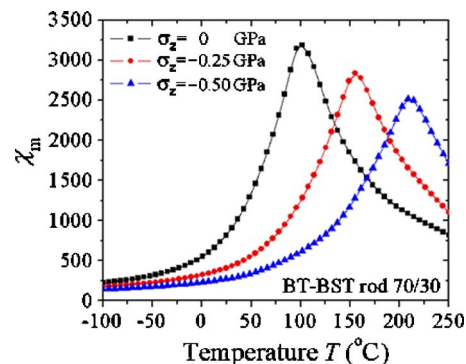


FIG. 2. (Color online) Mean dielectric susceptibility χ_m as a function of temperature T for the BST (70/30) CGFR in S-H-C system for different applied pressure.

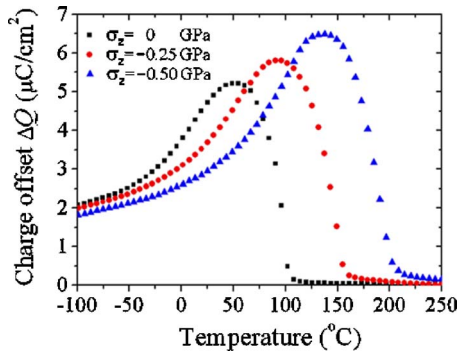


FIG. 3. (Color online) Charge offset ΔQ as a function of temperature in BST (70/30) rod for different applied pressures.

achieved over a much larger range of operating temperatures.

The polarization profile along the z direction can be used to calculate the charge offset per unit area ΔQ according to the one-dimensional Poisson's equation,

$$\Delta Q = \frac{1}{L} \int_0^L z \left(\frac{dP(z)}{dz} \right) dz. \quad (4)$$

The charge offset has a strong temperature dependence, which has been confirmed both theoretically and experimentally.¹ This is described by an effective pyroelectric coefficient that can be defined as

$$p_{\text{eff}} = \frac{d\Delta Q}{dT} = \frac{1}{L} \frac{d}{dT} \int_0^L z \left(\frac{dP(z)}{dz} \right) dz. \quad (5)$$

Since a ferroelectric hysteresis loop can be observed by a Sawyer-Tower circuit, Eqs. (4) and (5) can be rewritten as $\Delta Q = C_Q / LC_F \int_0^L z [dP(z)/dz] dz$ and $p_{\text{eff}} = d\Delta Q/dT = C_Q / LC_F d[\int_0^L z [dP(z)/dz] dz]/dT$, where C_Q is the load capacitance in the Sawyer-Tower circuit and C_F is the capacitance of the ferroelectric.¹

Using Eqs. (4) and (5), the charge offset per unit area and the effective pyroelectric coefficient as a function of temperature and applied pressure are calculated and shown in Fig. 3. It is interesting that the charge offset can be tuned very effectively by adjusting the applied pressure. Figure 3 also shows the existence of an applied pressure-dependent temperature T_{max} , at which the charge offset peaks (58 °C for $\sigma_z = 0$ GPa, 95 °C for $\sigma_z = -0.25$ GPa, and 137 °C for $\sigma_z = -0.5$ GPa). The effective pyroelectric coefficient as a function of temperature is shown in Fig. 4, from which the effects of temperature and applied pressure on the CGF rod are obvious. In total, the results shown from Figs. 1–4 clearly show the high sensitivity of the polarization, charge offset, dielectric and pyroelectric properties of a CGF rod in an S-H-C arrangement to ambient temperature and applied pressure. This indicates the feasibility of controlling the properties of the rod for design optimization via adjustment of the applied pressure.

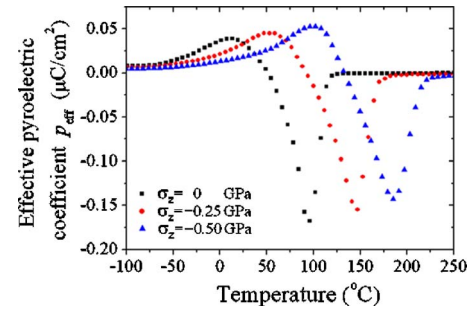


FIG. 4. (Color online) Effective pyroelectric coefficient p_{eff} as a function of temperature in BST (70/30) rod for different applied pressures.

In summary, a general model for CGFR is formulated using a thermodynamic approach based on the Landau-Ginsburg-Davenshire functional. The calculated distribution of the polarization in the rod, the corresponding charge offset, dielectric and pyroelectric properties are found to be highly sensitive to the applied pressure. Our results indicate that this behavior may provide a useful means of control of the properties of CGFR for design optimization.

This project was supported by Grants PolyU5312/03E and 5322/04E. B.W. is also grateful for support from the National Natural Science Foundation of China (Nos. 50232030, 10172030, and 10572155) and the Science Foundation of Guangzhou Province (2005A10602002).

- ¹S. Zhong, S. P. Alpay, Z.-G. Ban, and J. V. Mantese, *Appl. Phys. Lett.* **86**, 092903 (2005).
- ²N. W. Schubring, J. V. Mantese, A. L. Micheli, A. B. Catalan, and R. J. Lopez, *Phys. Rev. Lett.* **68**, 1778 (1992).
- ³S. Zhong, S. P. Alpay, Z.-G. Ban, and J. V. Mantese, *Integr. Ferroelectr.* **71**, 1 (2005).
- ⁴Z.-G. Ban, S. P. Alpay, and J. V. Mantese, *Phys. Rev. B* **67**, 184104 (2003).
- ⁵Z.-G. Ban, S. P. Alpay, and J. V. Mantese, *Integr. Ferroelectr.* **58**, 1281 (2003).
- ⁶J. V. Mantese, N. W. Schubring, A. L. Micheli, M. P. Thompson, R. Naik, G. W. Auner, I. B. Misirlioglu, and S. P. Alpay, *Appl. Phys. Lett.* **81**, 1068 (2002).
- ⁷W. Fellberg, J. Mantese, N. Schubring, and A. Micheli, *Appl. Phys. Lett.* **78**, 524 (2001).
- ⁸T. Granzow, A. B. Kounga, E. Aulbach, and J. Rodel, *Appl. Phys. Lett.* **88**, 252907 (2006).
- ⁹A. B. K. Njiwa, E. Aulbach, T. Granzow, and J. Rodel, *Acta Mater.* **55**, 675 (2006).
- ¹⁰A. N. Morozovska, E. A. Eliseev, and M. D. Glinchuk, *Phys. Rev. B* **73**, 214106 (2006).
- ¹¹G. Liu and C. W. Nan, *J. Phys. D* **38**, 584 (2005).
- ¹²B. Wang and C. H. Woo, *J. Appl. Phys.* **100**, 044114 (2006).
- ¹³Y. Zheng, B. Wang, and C. H. Woo, *Appl. Phys. Lett.* **89**, 062904 (2006).
- ¹⁴Y. Zheng, B. Wang, and C. H. Woo, *Appl. Phys. Lett.* **89**, 083115 (2006).
- ¹⁵J. V. Mantese and S. P. Alpay, *Graded Ferroelectrics Transpacitors and Transponents* (Springer, Berlin, 2005), pp. 52–54.
- ¹⁶In SI units for $\text{Ba}_x\text{Sr}_{1-x}\text{TiO}_3$, $\alpha = 1.12 \times 10^7 (T - 371x + 253) / (9x + 8)$, $\beta = (-11.96x + 8.4) \times 10^9$, $\gamma = 2.7 \times 10^{11}$, $C_{11} = (3.48 - 1.72x) \times 10^{11}$, $C_{12} = (1 - 0.154x) \times 10^{11}$, and $Q_{12} = -0.034$; data from Refs. 15 and 16.